Supporting Information

Highly-Efficient Charge Separation and Polaron Delocalization in Polymer-Fullerene Bulk-Heterojunctions: A Comparative Multi-Frequency EPR & DFT Study

Jens Niklas,[†] Kristy L. Mardis,[#] Brian P. Banks,[#] Gregory M. Grooms,[#] Andreas Sperlich,[‡] Vladimir Dyakonov,[‡]

Serge Beaupré[‡‡], Mario Leclerc[‡‡], Tao Xu, [§] Luping Yu,[§] Oleg G. Poluektov[†,*]

[†] Chemical Sciences and Engineering Division, Argonne National Laboratory, Argonne, Illinois 60439

[#] Department of Chemistry and Physics, Chicago State University, Chicago, Illinois 60628

[‡] University of Würzburg and Bavarian Centre for Applied Energy Research, D-97074 Würzburg, Germany

[‡‡] Department of Chemistry, Université Laval, Quebec City, Quebec, G1V 0A6, Canada

[§] Department of Chemistry and James Franck Institute, University of Chicago, Chicago, Illinois 60637

Device preparation

Bulk-Heterojunction (BHJ) solar cells were prepared by spin coating a 35 nm layer of PEDOT:PSS (Clevios P VP AI 4083) on indium tin oxide (ITO) samples with a post-annealing step of 130 °C for 10 minutes. The organic blend solutions were solved in chlorobenzene (see Table S1 for weight ratios). For the PTB7:C_{70}-PCBM blend 3 vol-% 1,8-diiodoctane (DIO) were added to obtain smoother films. The solutions were spun in a nitrogen glove box system resulting in about 120 nm thick layers. The P3HT:fullerene films were thermally treated at 130 °C and PCDTBT:C_{70}-PCBM films at 50 °C for 10 minutes before metal deposition. Ca/Al was thermally evaporated on top of the active layer. The current–voltage (I-V) characteristics of the organic solar cells were measured under anaerobic conditions in a nitrogen glove box system. We used an Oriel 1160 AM1.5G solar simulator for illumination.

Table S1. Characteristic parameters of the polymer:fullerene BHJ solar cells with blending weight ratio, open-circuit voltage (V_{OC}), short-circuit current (J_{SC}), fill factor (FF) and calculated power conversion efficiency (PCE).

	weight ratio	V_{OC} (mV)	J_{SC} (mA/cm^2)	FF (%)	PCE (%)
P3HT:C_{60}-PCBM	1:0.8	565	8.31	70	3.27
P3HT:C_{70}-PCBM	1:0.8	560	9.43	62	3.25
PCDTBT:C_{70}-PCBM	1:4	905	10.0	66	6.12
PTB7:C_{70}-PCBM	1:1.5	718	14.61	69	7.26

P3HT

Table S2. The principal values of the g-tensor of the positive, P^+, polarons on P3HT oligomers as obtained by DFT calculations. All oligomers have dihedral values of 180° ("trans") as shown in Figure 4 unless explicitly labeled "cis" (dihedral = 0°). The energy difference between the cis and trans conformers of same length for the hexyl/EPRII cases are +2.8, +2.2, and +4.2 kcal/mol, for the dimer, trimer, and pentamer respectively ($E_{cis\ conformer} > E_{trans\text{-}conformer}$). Figure S2 gives a graphical representation of data selected from this Table. Figure S1 depicts spin density plots of tetramers with different sidechains. The functional was in all cases B3LYP[1-4] in combination with the def2-TZVPP basis set[5-7] for ^{32}S. Different basis sets (def2-TZVPP or EPRII[8,9]) were used for the lighter atoms (^{12}C, ^{1}H). Further details of the calculations are provided in Experimental Procedures.

Basis	*def2-TZVPP (all atoms)*			*EPRII (def2-TZVPP for ^{32}S)*			*EPRII (def2-TZVPP for ^{32}S)*			*EPRII (def2-TZVPP for ^{32}S)*		
Substituent	Hexyl			Hexyl			Hydrogen			Methyl		
Chain Length	g_Z	g_Y	g_X	g_Z	g_Y	g_X	g_Z	g_Y	g_X	g_Z	g_Y	g_X
1	2.0007	2.0021	2.0056	2.0007	2.0020	2.0056	2.0006	2.0020	2.0021			
2	2.0005	2.0021	2.0042	2.0005	2.0021	2.0041	2.0003	2.0021	2.0045	2.0004	2.0021	2.0041
2-cis	2.0010	2.0023	2.0041	2.0010	2.0023	2.0039	2.0009	2.0021	2.0033	2.0012	2.0021	2.0038
3	2.0015	2.0022	2.0030	2.0016	2.0022	2.0028	2.0016	2.0022	2.0027			
3-cis	2.0003	2.0022	2.0042	2.0005	2.0022	2.0039	2.0003	2.0022	2.0036			
4	2.0010	2.0022	2.0033	2.0011	2.0022	2.0030	2.0010	2.0022	2.0030	2.0010	2.0022	2.0030
5	2.0011	2.0023	2.0029	2.0012	2.0022	2.0027	2.0010	2.0022	2.0026			
5-cis	2.0005	2.0026	2.0033				1.9999	2.0023	2.0035			
6	2.0008	2.0023	2.0030	2.0009	2.0022	2.0027	2.0007	2.0022	2.0026			
7				2.0008	2.0023	2.0027	2.0006	2.0022	2.0026			
8				2.0006	2.0022	2.0027	2.0004	2.0022	2.0025	2.0005	2.0022	2.0026
9							2.0003	2.0022	2.0025			
12							2.0001	2.0022	2.0025			
13							2.0001	2.0022	2.0025	2.0002	2.0022	2.0025
15							2.0014	2.0023	2.0026			
18							2.0002	2.0023	2.0026			

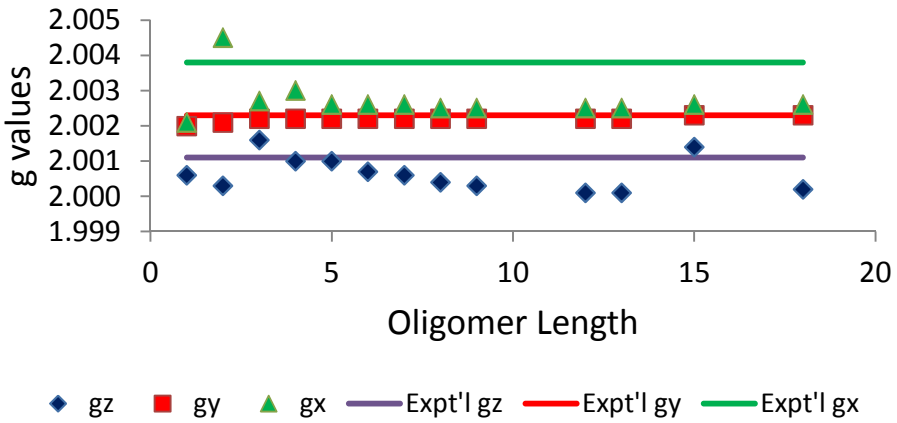

Figure S1. Calculated principal values of the *g*-tensor of positive, P^+, polarons on P3HT oligomers (trans conformer, dihedral = 180°) as a function of oligomer length (see Table S1 for a more comprehensive data set). The hexyl sidechain was replaced by hydrogen; B3LYP functional; def2-TZVPP basis set for ^{32}S, EPRII basis set for ^{12}C and ^{1}H. The *g*-values values are generally insensitive to oligomer length. The principal *g*-value g_X is generally underestimated by approximately $12*10^{-4}$ when compared to the experimental values. Comparison of the different calculations on the smaller oligomer models suggests that using a def-TZVPP basis for all atoms on the hexyl sidechain containing P3HT model oligomer would reduce the deviation from the experimental values below $9*10^{-4}$.

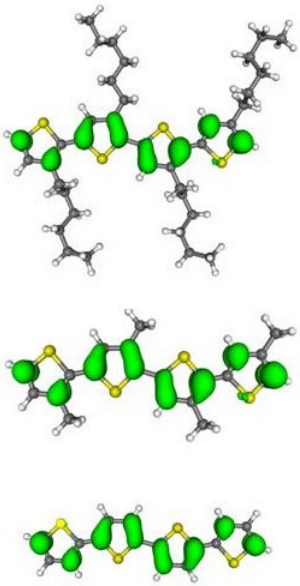

Figure S2. Spin density isosurface plot (contour level of 0.002 e/a_0^3) for the P3HT tetramer (trans conformer) with complete hexyl sidechains **(top)**, for the methyl substituted tetramer **(middle)**, and the hydrogen substituted tetramer **(bottom)**. B3LYP functional; def2-TZVPP basis set for ^{32}S, EPRII basis set for ^{12}C and ^{1}H. The spin density does not extend to the alkyl chain and is similar for all three molecules.

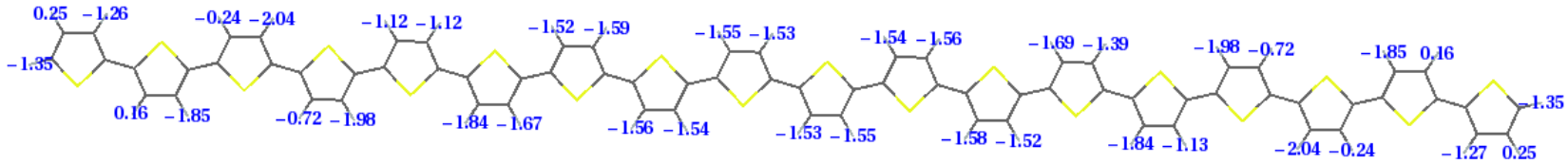

Figure S3. Calculated isotropic ^{1}H hyperfine coupling constants for the largest P3HT oligomer (18-mer). The overall charge on the complex is +1. B3LYP functional; def2-TZVPP basis set for ^{32}S, EPRII basis set for ^{12}C and ^{1}H. Further details of the calculations are provided in Experimental Procedures.

Table S2. The principal values of the ^{1}H hyperfine A-tensors (MHz) on the centermost thiophene unit of positive, P^{+}, polarons on oligomers of P3HT of various lengths as obtained by DFT calculations. Oligomers with odd units have only one unique value due to symmetry. Note, that principal axes of A-tensor and g-tensor are not necessarily identical. Further details of the calculations are provided in Experimental Procedures. A graphical representation and nomenclature is given in Figure S4.

Basis set	*def2-TZVPP (all atoms)*			*EPRII (def2-TZVPP for ^{32}S)*					
Side chain	Hexyl			Hexyl			Hydrogen		
	A_X	A_Y	A_Z	A_X	A_Y	A_Z	A_X	A_Y	A_Z
Monomer	1.2073	4.7331	6.8582	1.8364	5.0339	7.2352	2.0793	-10.3715	-12.7121
Dimer-Ha	0.5117	-0.8975	3.8625	-0.6801	0.7148	4.0402	-1.5108	-2.2196	3.6838
Dimer-Hb	-2.6254	-12.0444	-16.5743	-3.4874	-13.6370	-17.7186	-3.5922	-14.1944	-18.4535
Dimer-cis-Ha	-0.6366	1.0703	3.8099	-0.4008	1.2802	3.9972	-.5112	-1.6015	4.0548
Dimer-cis-Hb	-2.1323	-10.2785	-13.2726	-2.7730	-11.5357	-14.1277	-4.1895	-15.1094	-18.9902
Trimer	-0.1586	-6.3468	-8.0070	-0.5196	-7.0383	-8.4617	-0.5455	-7.5589	-9.1111
Trimer-cis	-0.0645	-5.6192	-6.4042	-0.3426	-6.1974	-6.7681	-0.6764	-7.4126	-8.1602
Tetra-Hb	-2.2183	-8.6981	-12.5411	-2.7811	-9.8145	-13.2588	-2.1517	-8.8120	-11.6270
Tetra-Ha	0.9042	-3.0346	-3.1762	0.7827	-3.2960	-3.3504	0.8819	-3.8643	-4.0276[a]
Penta	-0.9083	-5.5681	-7.6921	-1.2324	-6.2229	-8.0871	-0.7059	-5.7358	-7.1987
Hexa-Ha				-0.3855	-4.0253	-4.9570	0.1071	-3.7824	-4.4303
Hexa-Hb				-2.1169	-7.4401	-10.1120	-1.4630	-6.3703	-8.4280
Hepta				0.0167	-2.7333	-3.1669	-0.6798	-4.7061	-6.0027
Octa-Hb				-1.7904	-6.1544	-8.4170	-1.0987	-5.0362	-6.6483
Octa-Ha				-0.6924	-4.0079	-5.1465	-0.1870	-3.5324	-4.3234[b]
Non							-0.6272	-4.0054	-5.1462
Twelve-Hb							-0.6666	-3.3664	-4.3794
Twelve-Ha							-0.3891	-2.9103	-3.6720
Thirteen							-0.5034	-2.9199	-3.7428[c]
Fifteen							-0.4340	-2.4542	-3.1253
Eighteen-Ha							-0.3376	-1.8819	-2.3764
Eighteen-Hb							-0.3480	-1.9009	-2.4038

[a]The tetramer methyl values are Ha: -2.5645, -9.4719, -12.7197 and Hb: 0.6342, -3.4857, -3.6650

[b] the octamer methyl values are Ha -0.5792, -3.7497, -4.7993 and Hb: -1.6517, -5.8655, -8.0097;

[c] the thirteenmer methyl values are -1.0221, -3.6744, -4.9861; the thirteenmer ethyl values are -0.9900, -3.6226, -4.8943

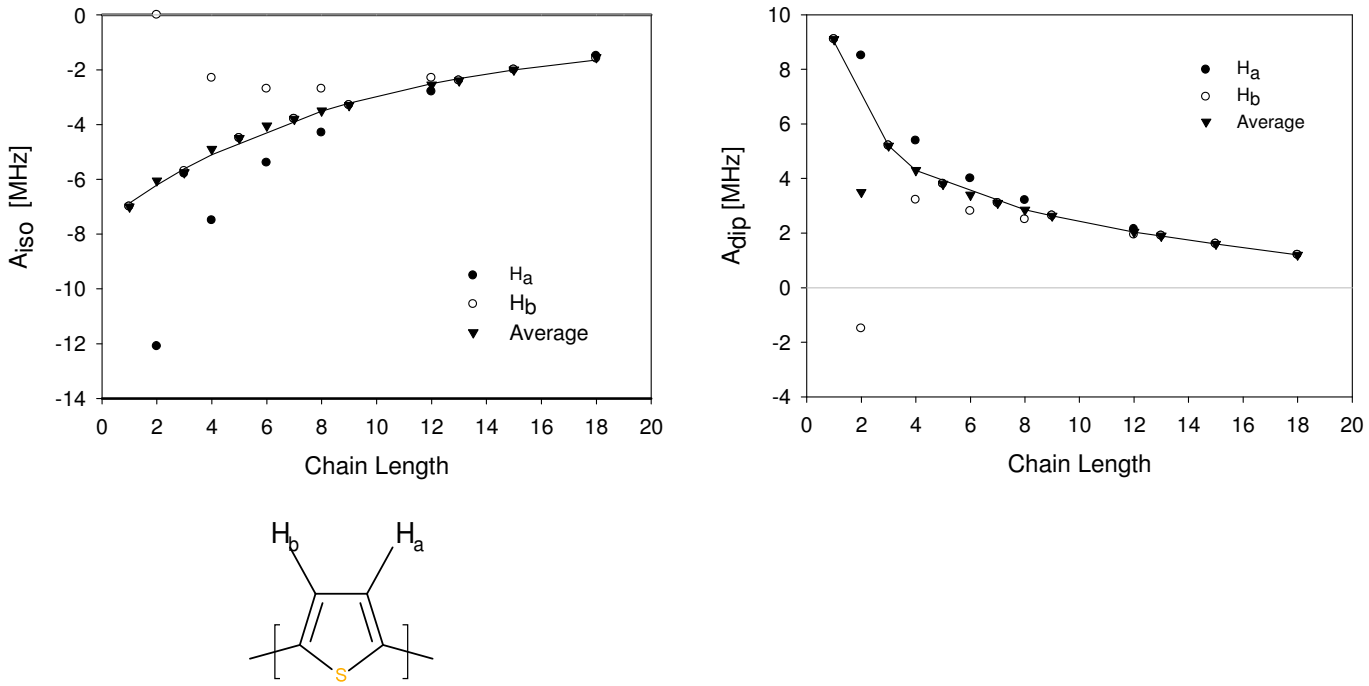

Figure S4. ^{1}H hyperfine coupling constants for the centermost hydrogen atoms on the P3HT oligomer as a function of oligomer length, using selected data from Table S2. The overall charge on the complex is +1. Even numbered oligomers are not symmetric and have two values (H_a and H_b - see below), odd numbered oligomers are symmetric and the ^{1}H hyperfine coupling constants both hydrogen atoms are identical. The functional was B3LYP. The basis set def2-TZVPP was used for ^{32}S, while the EPRII basis set was used for the lighter atoms (^{12}C, ^{1}H). **Left.** Isotropic part of the ^{1}H hyperfine coupling constants. **Right.** Largest component of the dipolar part of the ^{1}H hyperfine coupling tensor.

Table S3. DFT calculations on a stacked dimer of a trimeric P3HT oligomer (see Figure S5). Sidechains have been truncated to ethyl groups. The overall charge on the complex is +1. The *g*-values show only minor differences as compared to the unbound trimer, and do not depend significantly on the distance of the two stacked oligomers, the largest effect is seen on the g_Z-values. The orientation of the g-tensor principal axes is hardly changed in the stacked oligomer. The ^{1}H hyperfine coupling constants of the two central hydrogen atoms of the single trimer are decreased approximately by a factor of 2 in the stacked trimer, but do not depend strongly on the distance in the range 3.80-3.95Å. The orientation of the ^{1}H hyperfine coupling tensor principal axes is hardly changed in the stacked dimer as compared to the isolated oligomer. Both in the stacked system and in the isolated trimer the ^{1}H hyperfine coupling tensor principal axes deviate significantly from co-linearity with the principal axes of the g-tensor. The same statements hold for the second oligomer. Further details of the calculations are provided in Experimental Procedures.

Distance between two trimers (Å)[#]	g_Z	g_Y	g_X	*ΔE(kcal/mol)*	A_X	A_Y	A_Z	A_X (MHz)	A_Y	A_Z
3.80	2.00192	2.00236	2.00312	0.34	0.2833	-3.2488	-3.7562	0.1108	-2.2122	-3.0290
3.85	2.00197	2.00223	2.00307	0.30	0.3190	-3.1802	-3.6545	0.1197	-2.2099	-3.0243
3.90	2.00194	2.00224	2.00308	0.03	0.2773	-3.3000	-3.8264	0.0924	-2.1793	-3.0051
3.95	2.00222	2.00230	2.00295	---	0.3502	-3.1025	-3.5539	0.1296	-2.2189	-2.9981
∞	2.00160	2.00220	2.00277		-0.7129	-7.3181	-8.8927	-0.7129	-7.3181	-8.8927

[#] Distance as defined in Figure S5.

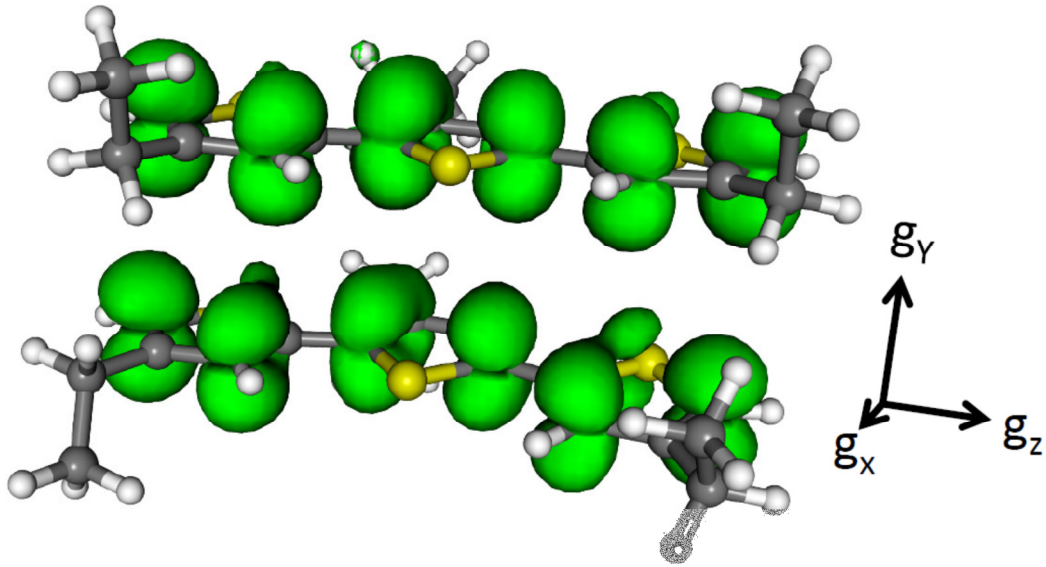

Figure S5. Spin density isosurface plot of a stacked dimer of a trimeric oligomer of P3HT with the distance between the layers constrained to 3.85 Å (distance between the two hydrogen atoms of the central thiophene). Sidechains are truncated to ethyl groups. The overall charge on the complex is +1. The orientation of the principal axes of the electronic g-tensor is also given; it is hardly changed in the stacked oligomer as compared to the isolated trimer. The orientation of the ^{1}H hyperfine coupling tensor principal axes is hardly changed in the stacked dimer as compared to the isolated oligomer. Both in the stacked system and in the isolated trimer the ^{1}H hyperfine coupling tensor principal axes deviate significantly from co-linearity with the principal axes of the g-tensor. The same statements hold for the second oligomer. All isosurfaces are shown at a contour level of 0.0005 e/a_0^3. Energy and magnetic resonance parameters for this and different distances are given in Table S3. Further details of the calculations are provided in Experimental Procedures.

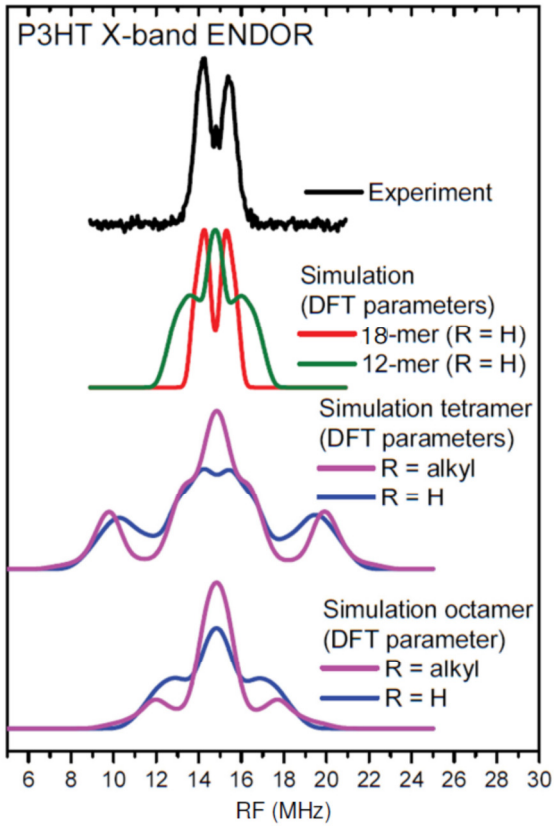

Figure S6. Light-induced Davies-type[10,11] ENDOR spectrum of P3HT:C_{60}-PCBM blends at cryogenic temperatures. Black – experiment. Red –simulation based on DFT calculations done for: 18-mer of P3HT cation; Green – simulation based on DFT calculations of 12-mer P3HT; Magenta – simulation based on DFT calculations of tetramer/octamer P3HT with hexyl sidechain; Blue – simulation based on DFT calculations of tetramer/octamer P3HT with hydrogen replacing the hexyl sidechain. Note, that replacing the hexyl sidechain by hydrogen has negligible influence on the spread of the ENDOR spectra. The simulation based on DFT calculations of 18-mer P3HT agrees very well with the experimental ENDOR spectrum, while the simulation based on DFT calculations of 12-mer P3HT shows a too wide ENDOR spectrum.

PCDTBT

Table S4. The principal values of the g-tensor of positive, P^+, polarons on various PCDTBT model monomers. Two conformations with a range of substituents on the nitrogen atom were investigated (see below). Little effect on the g-tensor and the ^1H hyperfine coupling tensors was seen. Further details of the calculations are provided in Experimental Procedures.

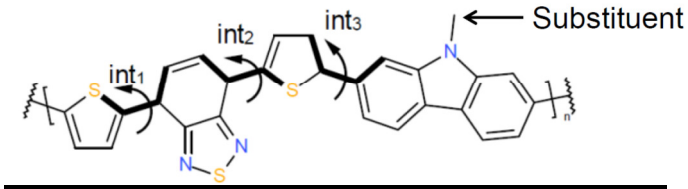

Dihedral (deg.) int1,int2,int3	*Substituent*	g_Z	g_Y	g_X
0, 180, 180	Methyl	2.0012	2.0023	2.0030
0, 180, 180	Isopropyl	2.0012	2.0023	2.0031
0, 180, 180	di-octyl	2.0013	2.0024	2.0031
180, 0, 0	Methyl	2.0011	2.0023	2.0030
180, 0, 0	isopropyl	2.0011	2.0023	2.0029
180, 0, 0	di-octyl	2.0020	2.0024	2.0028

Table S5. The principal values of the g-tensor of positive, P^+, polarons on the PCDTBT model monomer (methyl substituent, see above). Little change in the g-tensor values is seen upon changing the conformation of the oligomer or upon increasing the size of the polymer. B3LYP functional; def2-TZVPP basis set for ^{32}S, EPRII basis set for ^{14}N, ^{12}C and ^{1}H. Energies are given relative to the lowest energy conformer of this length. Further details of the calculations are provided in the Experimental Procedures.

	Dihedrals (deg.) int1,int2,int3 [external]	g_Z	g_Y	g_X	ΔE *(kcal/mol)*
Monomer	0, 180, 0	2.0012	2.0023	2.0030	---
Monomer	0, 180, 180	2.0019	2.0023	2.0029	0.04
Monomer	180,180,180	2.0010	2.0023	2.0034	0.21
Monomer	180,180,0	2.0010	2.0023	2.0034	0.29
Monomer	0, 0, 0	2.0012	2.0023	2.0031	0.40
Monomer	0,0,180	2.0012	2.0023	2.0037	0.46
Monomer	180,0,0	2.0011	2.0023	2.0030	0.53
Monomer	180,0,180	2.0011	2.0023	2.0030	0.62
Dimer	0,180,0 [0]	2.0009	2.0024	2.0030	---
Dimer	0,180,0 [180]	2.0013	2.0023	2.0027	0.04
Dimer	0,180,180 [180]	2.0009	2.0023	2.0030	0.39
Dimer	0,180,180 [0]	2.0013	2.0023	2.0026	0.45
Dimer	180,180,180 [0]	2.0008	2.0025	2.0032	0.56
Dimer	180,180,180 [180]	2.0017	2.0023	2.0030	0.66
Dimer	0,0,180 [180]	2.0015	2.0024	2.0028	1.00
Dimer	0,0,180 [0]	2.0012	2.0023	2.0030	0.63
Trimer	0,0,0 [0,0]	2.0014	2.0024	2.0029	---
Trimer	0,0,0 [0,180]	2.0013	2.0024	2.0029	0.41
Trimer	0,0,0 [180,0]	2.0017	2.0024	2.0026	1.29
Trimer	0,0,0 [180,180]	2.0015	2.0024	2.0027	2.59
Trimer	0,180,180 [0,180]	2.0012	2.0023	2.0029	5.08
Trimer	0,180,180 [180,0]	2.0013	2.0023	2.0028	5.25
Trimer	0,180,1800 [0,0]	2.0015	2.0023	2.0025	6.48
Trimer	0,180,0 [0,180]	2.0015	2.0024	2.0026	7.24
Trimer	0,180,0 [180,0]	2.0012	2.0024	2.0029	7.76
Trimer	0,180,0 [180,180]	2.0015	2.0024	2.0027	8.31

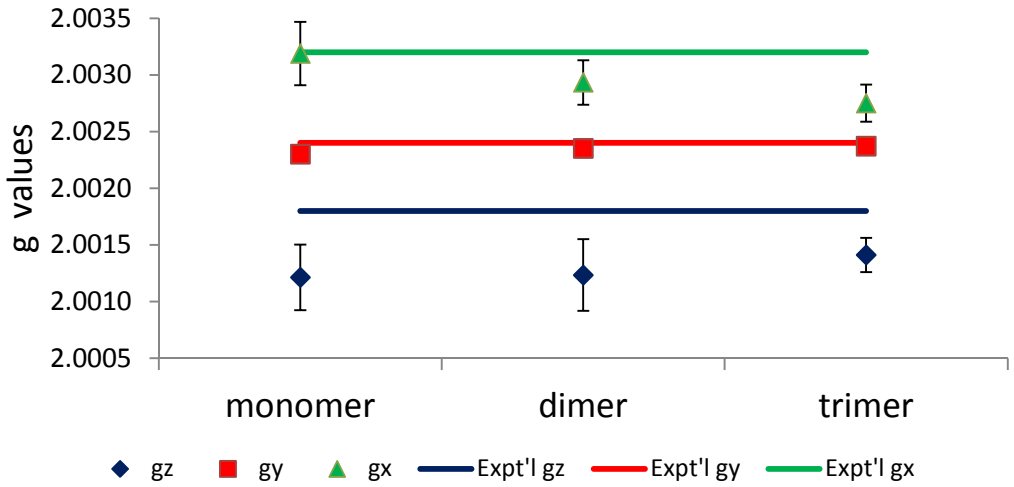

Figure S7. The principal values of the g-tensors of positive, P^+, polarons on PCDTBT model oligomers (methyl substituent, see above) averaged overall all conformers (standard deviation shown as error bars) as a function of oligomer length. B3LYP functional; def2-TZVPP basis set for ^{32}S, EPRII basis set for ^{14}N, ^{12}C and ^{1}H. Further details of the calculations are provided in the Experimental Procedures. These values are generally insensitive to oligomer length and, with the exception of g_Y, slightly underestimate the experimental values.

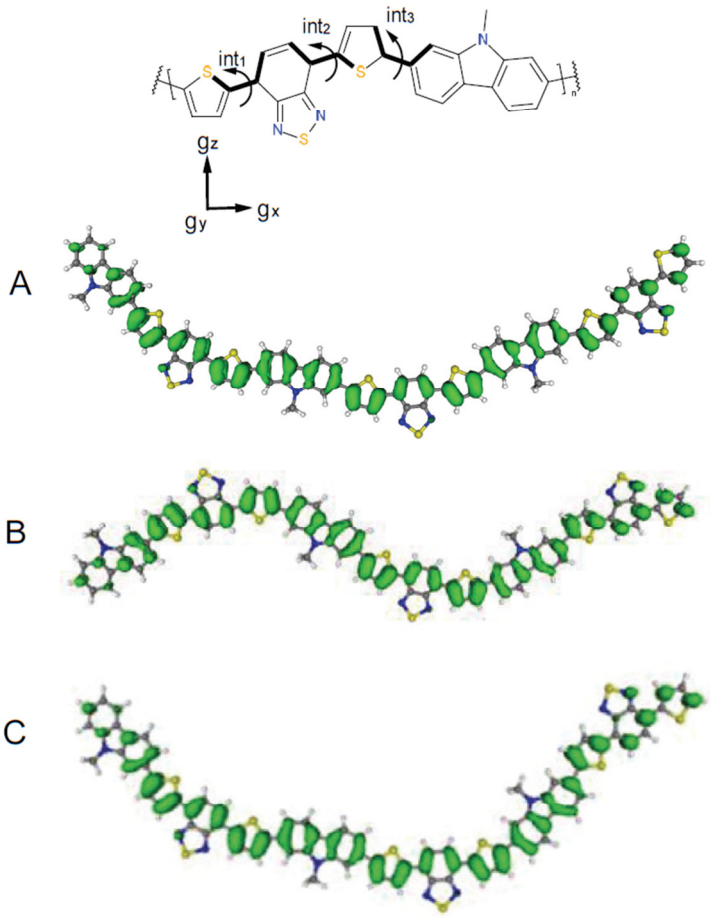

Figure S8. Spin density isosurface plots of several low energy conformers of the PCDTBT trimer. All isosurfaces are shown at a contour level of 0.0005 e/a_0^3. The orientation of the principal axes of the electronic g-tensor is also given. The arrows indicate the bonds which allow internal rotations. Table S5 shows the compilation of the energies of all calculated PCDTBT models. **A.** Lowest energy conformation. The three internal dihedral angles (int_1-int_3) are 0°, 0°, and 0° in each monomer, and the external angles are all 0°. **B.** Fourth lowest energy conformation. The three internal dihedral angles (int_1-int_3) are 0°, 0°, and 0° in each monomer, and the external angles are all 180°. **C.** Third lowest energy conformation. The three internal dihedral angles (int_1-int_3) are 0°, 0°, and 0° in each monomer, and the external angles are 180° and 0°.

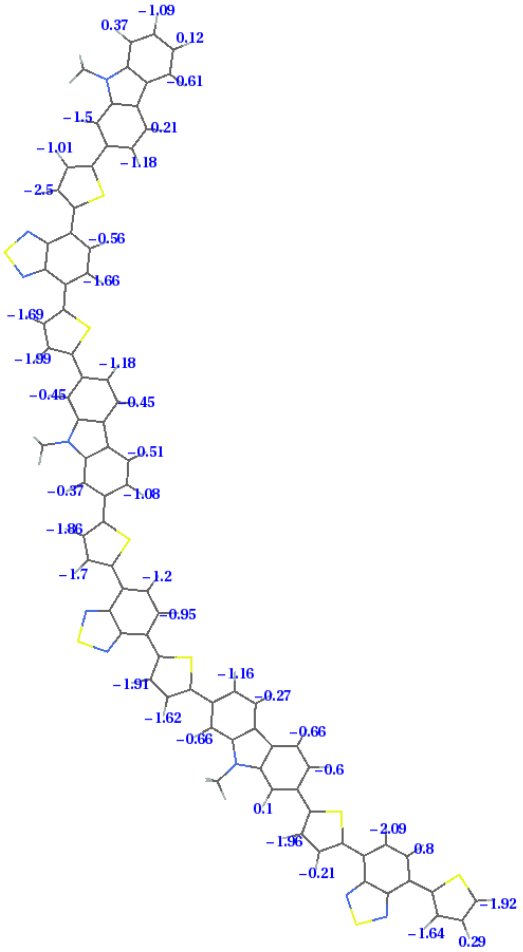

Figure S9. Calculated isotropic ^{1}H hyperfine coupling constants for the lowest energy trimer model structure of PCDTBT. B3LYP functional; def2-TZVPP basis set for ^{32}S, EPRII basis set for ^{14}N, ^{12}C and ^{1}H. Further details of the calculations are provided in Experimental Procedures.

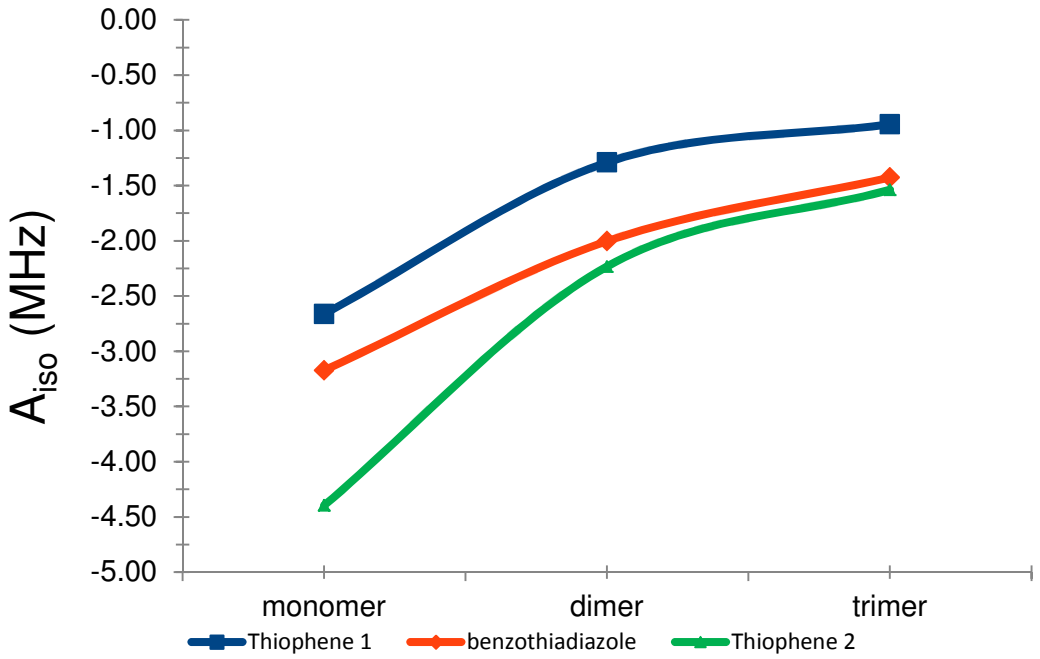

Figure S10. Calculated isotropic ^{1}H hyperfine coupling constants for ^{1}H for the lowest energy conformation of PCDTBT. The hyperfine constants are averaged over all hydrogen atoms on a particular group since the molecule is not symmetric. B3LYP functional; def2-TZVPP basis set for ^{32}S, EPRII basis set for ^{14}N, ^{12}C and ^{1}H. Further details of the calculations are provided in Experimental Procedures. The magnitude decreases as the oligomer length increases.

Table S6. The principal values of the g-tensor of negative, P^-, on the C_{70}-PCBM fullerenes, in PCDTBT:C_{70}-PCBM blends polymer-fullerenes blends in frozen toluene vs. chlorobenzene solution (see Figure S10).

g-tensor[a)]	P^- in PCDTBT:C_{70}-PCBM in toluene	P^- in PCDTBT:C_{70}-PCBM in chlorobenzene
g_X	2.0062	2.0057
g_Y	2.00265	2.00265
g_Z	2.0020	2.0020

[a)]Relative error in the g-tensor measurements is ±0.0001.

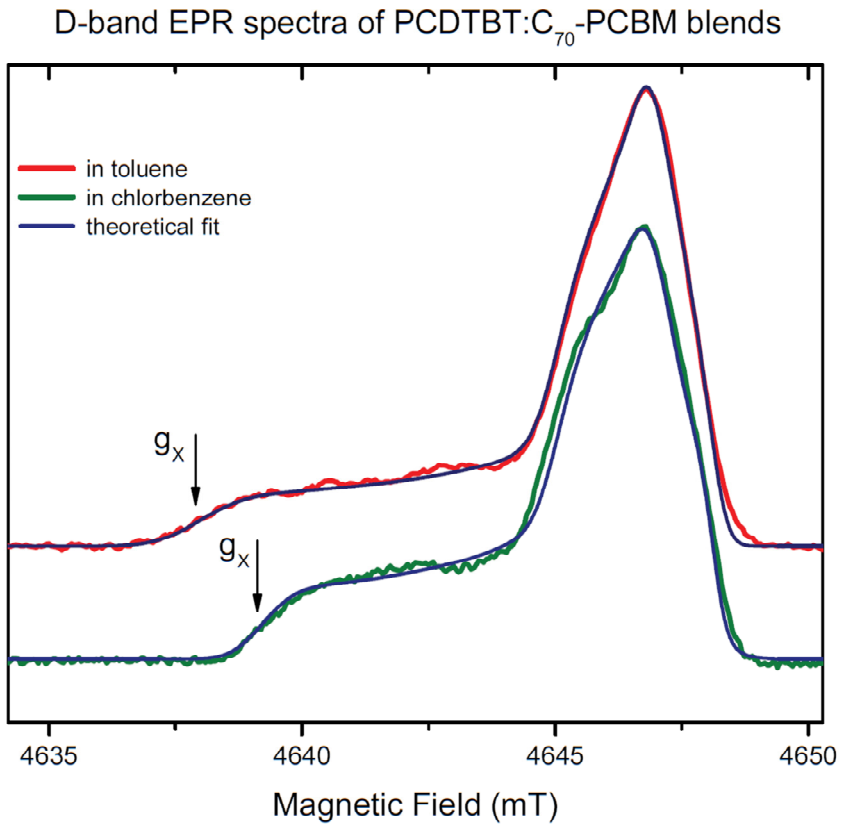

Figure S11. Echo-detected D-band EPR spectra of PCDTBT:C_{70}-PCBM blends using toluene (Red) or chlorobenzene (Green) as solvent. Illuminated at 50 K. Simulations of the experimental spectra are shown in Blue. The low field component of C_{70}-$PCBM^-$, g_X, exhibits a large g-strain effect, which reveals in the large linewidth of this component and indicates the sensitivity on its direct surrounding. Slight variations of g_X value, in the order of ±0.0002, were observed in different samples prepared in toluene solution. The use of chlorobenzene instead of toluene as solvent also had a slightly larger effect on this g-value. Table S6 provides the principal g-values of C_{70}-PCBM anions used for the simulation.

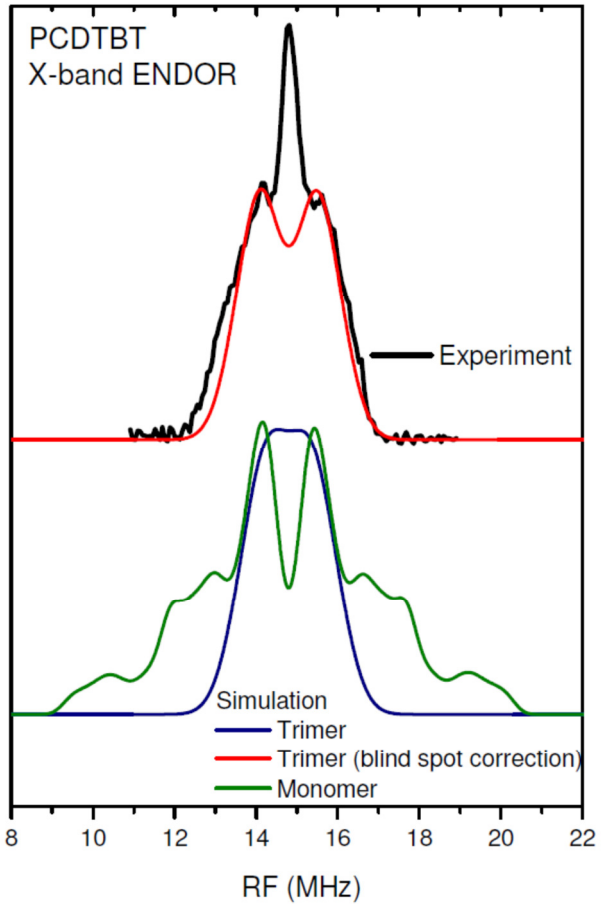

Figure S12. Light-induced Mims-type[10,11] ENDOR spectrum of PCDTBT:C_{60}-PCBM blends, recorded at cryogenic temperatures. Black – experiment. Blue – simulation based on DFT calculations done for trimer PCDTBT cation; Red –simulation based on DFT calculations done for trimer PCDTBT cation, corrected for blind spot according to ref.[10]; Green –simulation based on DFT calculations done for monomer PCDTBT cation. The simulation based on DFT calculations of timer PCDTBT agrees very well with the experimental ENDOR spectrum, while the simulation based on DFT calculations of monomer PCDTBT shows a far too wide ENDOR spectrum.

PTB7

Table S7. The principal values of the g-tensors of positive, P^+, polarons on PTB7 model oligomers of various length and conformations as obtained by DFT calculations. B3LYP functional; def2-TZVPP basis set for ^{32}S, EPRII basis set for ^{19}F, ^{12}C and ^{1}H. Energies are given relative to the lowest energy conformer of this length. Further details of the calculations are provided in Experimental Procedures.

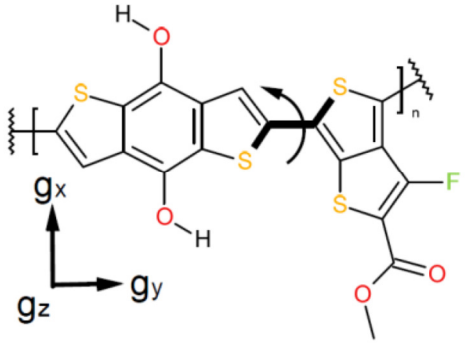

	Dihedrals (deg.) internal [external]	g_Z	g_Y	g_X	*ΔE (kcal/mol)*
Monomer	180	2.0023	2.0048	2.0073	---
Monomer	0	2.0022	2.0044	2.0066	1.2
Dimer	0 [0]	2.0023	2.0037	2.0048	0.9
Dimer	0 [180]	2.0023	2.0038	2.0046	1.3
Dimer	180 [0]	2.0023	2.0030	2.0039	---
Dimer	180 [180]	2.0023	2.0040	2.0057	1.8
Trimer	180 [180,180]	2.0023	2.0030	2.0056	1.5
Trimer	180 [0,0]	2.0023	2.0033	2.0051	---
Trimer	0 [180,180]	2.0024	2.0032	2.0045	1.8
Trimer	0 [0,0]	2.0024	2.0035	2.0040	0.6
Tetramer	0 [180,180,180]	2.0024	2.0032	2.0044	2.0
Tetramer	0 [0,0,0]	2.0024	2.0034	2.0040	0.2
Tetramer	180 [180,180,180]	2.0023	2.0028	2.0057	1.6
Tetramer	180 [0,0,0]	2.0023	2.0034	2.0049	---

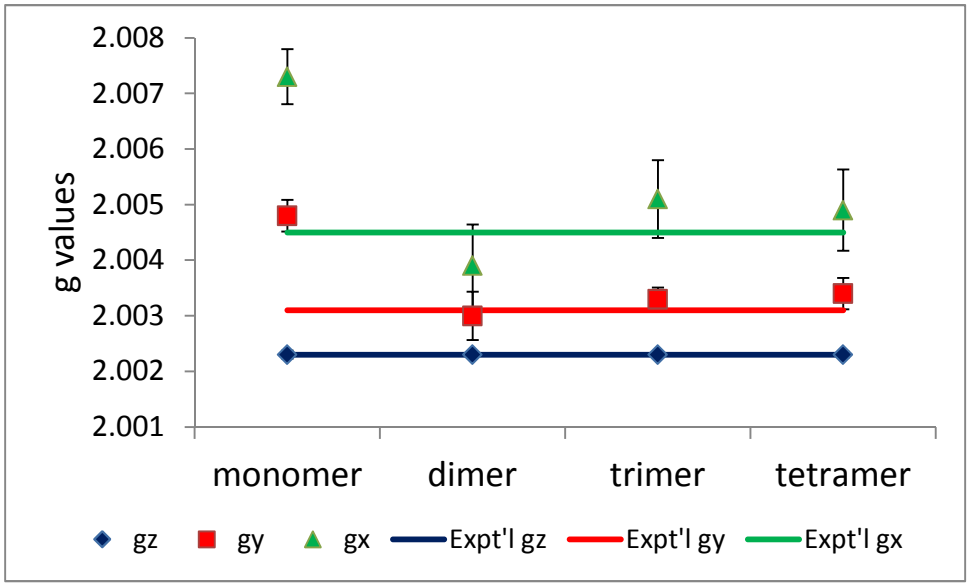

Figure S13. The principal values of the g-tensor of positive, P^+, polarons on PTB7 model oligomers averaged over all conformers for various lengths as obtained by DFT calculations. B3LYP functional; def2-TZVPP basis set for ^{32}S, EPRII basis set for ^{19}F, ^{12}C and ^{1}H. The experimental data are shown as solid lines, the standard deviation of calculated values for different conformers is shown by the error bars. While the monomer results agree poorly with experiment, smaller differences are apparent for larger oligomers and not trend as a function of oligomer size is present.

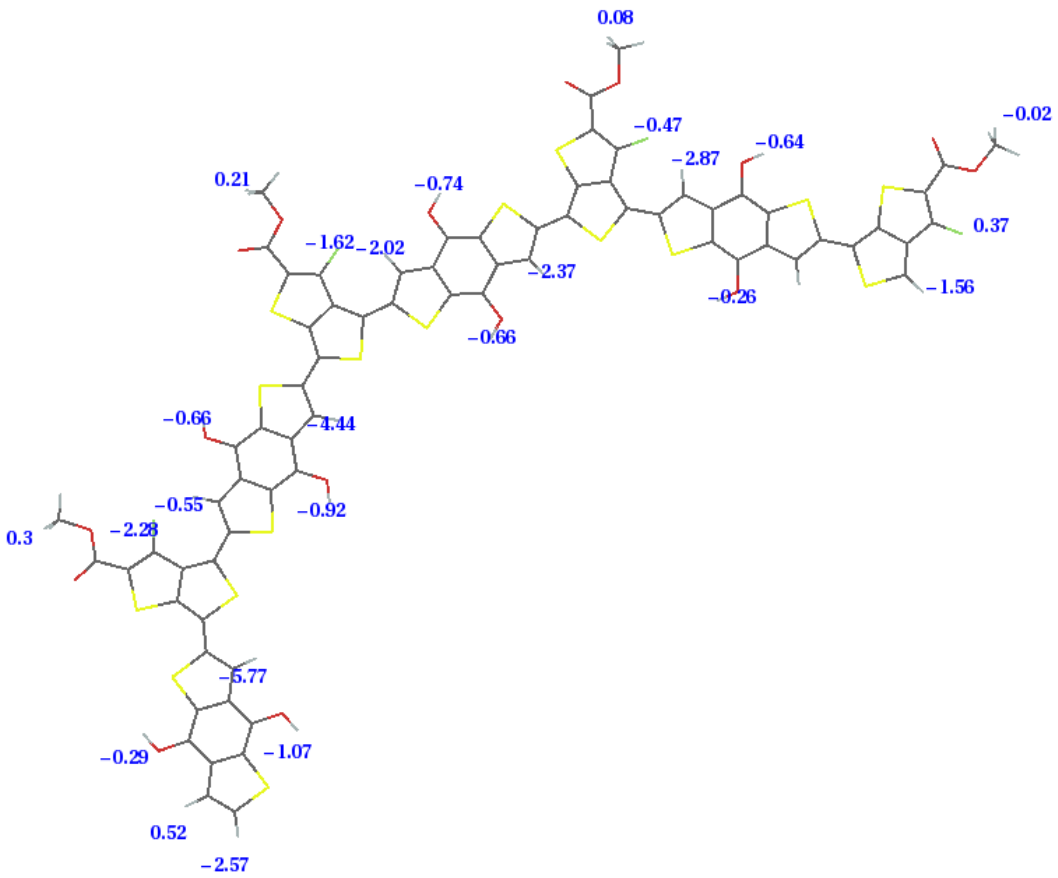

Figure S14. Calculated isotropic ^{1}H hyperfine coupling constants for ^{1}H and ^{19}F shown for the lowest energy tetramer model structure of PTB7. B3LYP functional; def2-TZVPP basis set for ^{32}S, EPRII basis set for ^{19}F, ^{12}C and ^{1}H. Further details of the calculations are provided in Experimental Procedures.

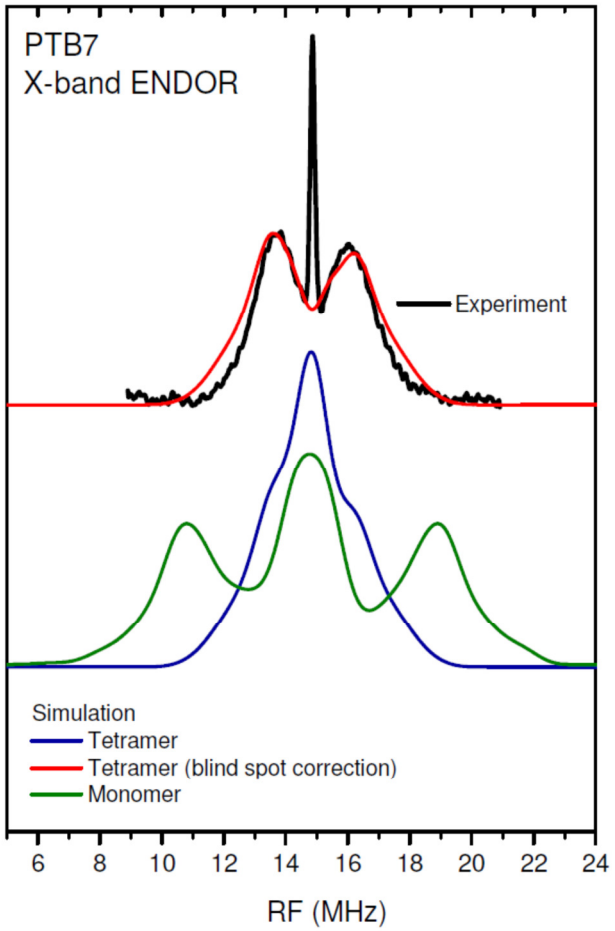

Figure S15. Light-induced Davies-type[10,12] ENDOR spectrum of PTB7:C_{60}-PCBM blends, recorded at cryogenic temperatures. Black – experiment. Blue – simulation based on DFT calculations done for tetramer PTB7 cation; Red –simulation based on DFT calculations done for tetramer PTB7 cation, corrected for blind spot according to ref.[10]; Green –simulation based on DFT calculations done for monomer PTB7 cation. The simulation based on DFT calculations of tetramer PTB7 agrees very well with the experimental ENDOR spectrum, while the simulation based on DFT calculations of monomer PTB7 shows a too wide ENDOR spectrum.

REFERENCES

(1) Becke, A. D. Density-Functional Thermochemistry .3. the Role of Exact Exchange. *Journal of Chemical Physics* **1993**, *98*, 5648-5652.

(2) Lee, C. T.; Yang, W. T.; Parr, R. G. Development of the Colle-Salvetti Correlation-Energy Formula into a Functional of the Electron-Density. *Phys. Rev. B* **1988**, *37*, 785-789.

(3) Vosko, S. H.; Wilk, L.; Nusair, M. Accurate Spin-Dependent Electron Liquid Correlation Energies for Local Spin-Density Calculations - a Critical Analysis. *Canadian Journal of Physics* **1980**, *58*, 1200-1211.

(4) Stephens, P. J.; Devlin, F. J.; Chabalowski, C. F.; Frisch, M. J. Ab-Initio Calculation of Vibrational Absorption and Circular-Dichroism Spectra Using Density-Functional Force-Fields. *Journal of Physical Chemistry* **1994**, *98*, 11623-11627.

(5) Weigend, F.; Ahlrichs, R. Balanced basis sets of split valence, triple zeta valence and quadruple zeta valence quality for H to Rn: Design and assessment of accuracy. *Physical Chemistry Chemical Physics* **2005**, *7*, 3297-3305.

(6) Schäfer, A.; Huber, C.; Ahlrichs, R. Fully Optimized Contracted Gaussian-Basis Sets of Triple Zeta Valence Quality for Atoms Li to Kr. *Journal of Chemical Physics* **1994**, *100*, 5829-5835.

(7) Schäfer, A.; Horn, H.; Ahlrichs, R. Fully Optimized Contracted Gaussian-Basis Sets for Atoms Li to Kr. *Journal of Chemical Physics* **1992**, *97*, 2571-2577.

(8) Rega, N.; Cossi, M.; Barone, V. Development and validation of reliable quantum mechanical approaches for the study of free radicals in solution. *Journal of Chemical Physics* **1996**, *105*, 11060-11067.

(9) Barone, V. Structure, Magnetic Properties and Reactivities of Open-Shell Species from Density Functional and Self-Consistent Hybrid Methods. In *Recent Advances in Density Functional Methods (Part 1)*; Chong, D. P., Ed.; World Scientific: Singapore, 1995; pp 287-334.

(10) Gemperle, C.; Schweiger, A. Pulsed Electron-Nuclear Double Resonance Methodology. *Chem. Rev.* **1991**, *91*, 1481-1505.

(11) Mims, W. B. Pulsed ENDOR Experiments. *Proceedings of the Royal Society of London Series A-Mathematical and Physical Sciences* **1965**, *283*, 452-457.

(12) Davies, E. R. A New Pulse ENDOR Technique. *Physics Letters* **1974**, *47A*, 1-2.